

Performance Analysis of QAM Modulations Applied to the LINC Transmitter

Fernando J. Casadevall, *Member, IEEE*, and Antonio Valdovinos, *Student Member, IEEE*,

Abstract—Future mobile radiocommunications systems will use linear modulations because they show a higher spectrum efficiency than classical FM modulations. Furthermore, in order to use these modulations in hand-portable equipment, power efficiency is also requested for the power amplifiers. To obtain both power and spectrum efficiency, a LINC¹ transmitter can be considered. In this paper, we present an analysis of the effect of different types of imbalances between the parallel signal paths in a LINC transmitter. The system degradations are described in terms of adjacent channel rejection, (U_R). Classical raised cosine (Nyquist filtered) 4, 16, and 64 QAM modulation patterns are taken into account, and in all cases, upper bounds for adjacent channel rejection as function of the gain and phase imbalances as well as of the guard band between adjacent channels are presented. Moreover, the impact of these imbalances in the system performance, characterized by means of the signal-to-noise ratio (SNR) increment needed to maintain a fixed error rate, is also considered. The results show that gain and phase imbalance between both RF paths could be a serious limitation for the LINC transmitter performance.

I. INTRODUCTION

IN MOBILE radio systems, the relative inefficient use of the spectrum by existing types of FM modulations such as MSK, GMSK, TFM, etc., has resulted in crowding on the available channels. They are still widely used because their constant envelope property is appropriate for using power-efficient nonlinear amplifiers. However, in the next generations of digital cellular radio systems, the use of Quadrature Amplitude Modulation (QAM) patterns will be required, [1], because they have a higher spectrum efficiency than the previously mentioned FM modulations. But, since QAM presents a nonconstant envelope, it will be necessary to consider linear power amplifiers which are less efficient than the classical class-C power amplifiers currently in use with the FM-type modulations.

In order to achieve both spectrum and power efficiency, several classical linearizing techniques for power amplifiers have been proposed in the technical literature, [2]–[5]. These techniques are usually categorized as: Feed-forward, Feedback, Predistortion, and LINC transmitter. Among them, in our opinion, one of the most promising is the LINC transmitter,

Manuscript received December 20, 1991; revised February 18, 1992, and July 16, 1992. This paper was supported by the CICYT (Spain) under Grant TIC90714.

The authors are with the Department of Signal Theory and Communications, Universidad Polit cnica de Catalunya, Apdo. 30.002, 08080 Barcelona, Spain.

IEEE Log Number 9208915.

¹ Acronym for Linear amplification using Nonlinear Components

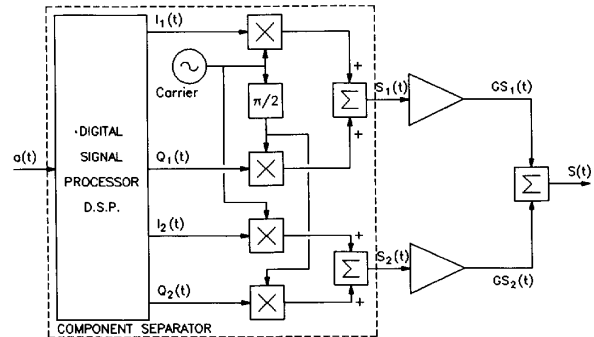


Fig. 1. Schematic diagram of the LINC transmitter.

because it does not use a feedback loop, thereby guaranteeing complete circuit stability.

The basic principle of the LINC transmitter is to represent any arbitrary bandpass signal, which may have both amplitude and phase variations, by means of two signals which are of constant amplitude and only have phase variations [5]. These two angle modulated signals can be amplified separately using efficient high-power nonlinear devices. Finally, the amplified signals are passively combined to produce an amplitude modulated signal. Fig. 1 shows the schematic drawing of such system where

$$\begin{aligned} S(t) &= G \cdot [a(t) \cdot \cos(\omega_0 t + \phi)] \\ S_1(t) &= V/2[\sin(\omega_0 t + \phi + \psi(t))] \\ S_2(t) &= V/2[\sin(\omega_0 t + \phi - \psi(t))] \end{aligned} \quad (1)$$

with $\psi(t) = \sin^{-1}[a(t)/V]$, and $\max[a(t)] \leq V$. Obviously, the component separator is a nonlinear device that could nowadays be implemented using digital signal processing (DSP) techniques.

In a practical LINC transmitter, there are several mechanisms that degrade the overall performance; e.g., the power gain and the delay (or phase) imbalance between the two RF paths or the errors due to the digital signal processing unit produces imperfect generation of the constant amplitude phase-modulated signal component, $S_1(t)$ and $S_2(t)$.

Some theoretical [7] and practical [6] works have been addressed to characterize the impact of these circuit malfunctions on the system performance considering the typical two tone as linearity test. However, to our knowledge, there is not yet a complete characterization of these effects when digital modulations are considered in which these degradations produce enhancement of the signal power spectrum that produces

TABLE I
VALUES OF THE V PARAMETER AS FUNCTION OF THE MODULATION PATTERN AND ROLL-OFF FACTOR

	4QAM			16QAM			64QAM		
	$A_x=0.9$	$A_x=0.6$	$A_x=0.3$	$A_x=0.9$	$A_x=0.6$	$A_x=0.3$	$A_x=0.9$	$A_x=0.6$	$A_x=0.3$
$\beta=0.2$	3.2490	5.8481	9.7469	9.7469	17.544	29.24	22.743	40.936	68.228
$\beta=0.5$	2.6388	4.7498	7.9163	7.9163	14.249	23.748	18.471	33.248	55.414
$\beta=0.7$	2.5745	4.9581	8.2635	8.2635	14.874	24.709	19.281	34.706	57.844
$\beta=0.9$	2.9460	5.3028	8.8379	8.8379	15.908	25.514	20.622	37.119	61.865

interference on the adjacent channels, thus limiting the system spectrum efficiency.

This paper presents an analysis of the effect of the errors on the system performance caused by the imbalance between the parallel RF paths. In particular, they have been characterized using two criteria: adjacent channel rejection (U_R), that is, the ratio between the power in the useful channel with respect to the power in the adjacent channel, and also by the signal-to-noise ratio (SNR) increment needed to maintain a fixed bit error rate (BER). 4, 16, and 64 QAM modulations patterns with square root raised cosine pulse shape have been considered. Moreover, the sensitivity to the gain and phase imbalances of a LINC transmitter have also been compared to the one obtained when a conventional QAM modulator is considered [8].

II. IMBALANCE ANALYSIS

An M -QAM modulated signal could be expressed as

$$S(t) = x(t) \cdot \cos(\omega_0 t) + y(t) \cdot \sin(\omega_0 t) \quad (2)$$

with

$$x(t) = \sum_{k=-\infty}^{\infty} a_k h_N^{0.5}(t - kT)$$

$$y(t) = \sum_{k=-\infty}^{\infty} b_k h_N^{0.5}(t - kT)$$

where $x(t)$ is the in-phase (I) component, $y(t)$ the quadrature (Q) component, $\{a_k\}$ and $\{b_k\}$ being the symbol sets transmitted in I and Q channels, $h_N^{0.5}(t)$ a square root raised cosine pulse shape, and T the symbol period.

After some algebraic effort from (1) and (2) it can be obtained:

$$S_1(t) = I_1(t) \cdot \cos(\omega_0 t) + Q_1(t) \cdot \sin(\omega_0 t)$$

$$S_2(t) = I_2(t) \cdot \cos(\omega_0 t) + Q_2(t) \cdot \sin(\omega_0 t) \quad (3)$$

$$I_1(t) = \frac{1}{2}[x(t) - C(t)y(t)]$$

$$Q_1(t) = \frac{1}{2}[C(t)x(t) + y(t)]$$

$$I_2(t) = \frac{1}{2}[x(t) + C(t)y(t)]$$

$$Q_2(t) = \frac{1}{2}[-C(t)x(t) + y(t)]$$

$$C(t) = \sqrt{\frac{V^2 - [x^2(t) + y^2(t)]}{x^2(t) + y^2(t)}}$$

For the roll-off factors and the QAM modulations considered in the paper, the V value is given in Table I using the ratio $A_x = \max[a(t)]/V$ as parameter, where $a(t)$ is the QAM signal envelope given by:

$$a(t) = \sqrt{x^2(t) + y^2(t)}$$

When the errors due to the RF processing are considered, the generated signal could be expressed as:

$$S(t) = G_1[I_1(t) \cos(\omega_0 t) + Q_1(t) \sin(\omega_0 t)] + G_2[I_2(t) \cos(\omega_0 t + \Delta\phi) + Q_2(t) \sin(\omega_0 t + \Delta\phi)]$$

where G_1 and G_2 are the voltage gain of each branch and $\Delta\phi$ is the phase imbalance between the two RF branches. Taking into account the expressions $I_1(t)$, $Q_1(t)$, $I_2(t)$, and $Q_2(t)$, the expression $S(t)$ results in

$$S(t) = G_1 \cdot [S_1(t) + S_2(t) + i(t)]$$

where

$$i(t) = \{\Delta G \cdot \sin(\Delta\phi) \cdot Q_2(t) - [1 - \Delta G \cdot \cos(\Delta\phi)] \cdot I_2(t)\} \cos(\omega_0 t) - \{\Delta G \cdot \sin(\Delta\phi) \cdot I_2(t) + [1 - \Delta G \cdot \cos(\Delta\phi)] \cdot Q_2(t)\} \sin(\omega_0 t)$$

is a residual interfering signal that appears due to the imbalances, and $\Delta G = G_2/G_1$. The signal $i(t)$ introduces interfering power in the adjacent channel limiting the spectrum efficiency of the system.

To analyze the effect of those imbalances, the power spectrum of the generated signal, $W(f)$, must be computed. In order to obtain $W(f)$, a pseudorandom sequence of 16384 QAM symbols is produced. With this sequence a set of 131 072 signal samples are generated. Eight samples per symbol period have been assumed. Then, the original sampled sequence is

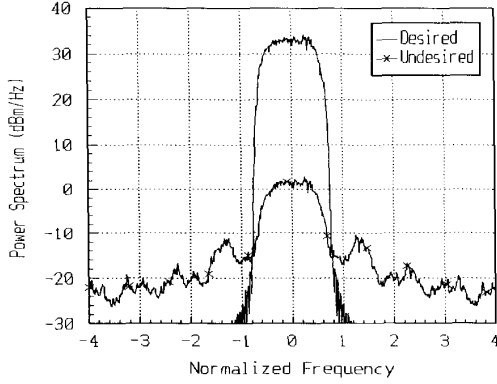


Fig. 2. Power Spectrum of 4-QAM pattern for a gain imbalance of 0.25 dB.

divided into 64 sequences with 2048 samples for each one. For each sequence the Fast Fourier Transform is evaluated using a Hanning window so as to decrease the side lobes. The final spectrum is computed as the average of the 64 spectra previously calculated.

In Fig. 2, the power spectrum for a raised cosine 4-QAM modulation with a roll-off factor equal to 0.5 is shown. A 0.25 dB of imbalance between both RF paths gain is taken into account. From the figure it can be seen that the undesired power spectrum extends further than the useful bandwidth, causing interference in the adjacent channels.

The adjacent channel rejection value, U_R , is obtained by means of the computation of the useful and interfering power using a numerical procedure. That is:

$$U_R(dB) = 10 \cdot \log_{10} \left[\frac{\int_{T_l}^{T_u} W(f) df}{\int_{I_l}^{I_u} W(f) df} \right]$$

being:

$$\begin{aligned} T_l &= -\left(\frac{1+\beta}{2T}\right) & T_u &= \left(\frac{1+\beta}{2T}\right) \\ I_l &= \left(\frac{1+\beta}{2T} + B_g\right) & I_u &= \left(\frac{1+\beta}{T} + I_l\right) \end{aligned}$$

where B_g is the guard band between the useful and the adjacent channel and β the roll-off parameter of the square root raised cosine filter.

III. RESULTS

A. Gain Imbalance

First of all, the evolution of the adjacent channel rejection, U_R (dB), against the gain imbalance has been studied using the roll-off factor as parameter and considering different values of the guard band between the adjacent channels. From the obtained results, it can be concluded that the system performances are almost insensitive to the roll-off value, whatever it is the QAM modulation considered. For this reason, from now on, only the roll-off value of 0.2, as typical

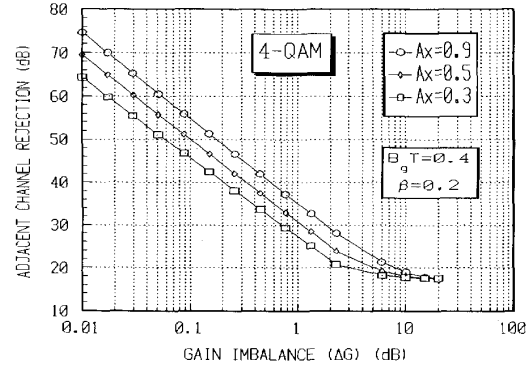


Fig. 3. Adjacent channel rejection versus the gain imbalance for 4-QAM modulation pattern with the amplitude of the phase modulated signals to the peak envelope value ratio as parameter.

for mobile radio communication systems, will be considered. Moreover, when the system performances for the different modulation patterns considered in the paper are compared, it is found that the differences in the adjacent channel rejection values are lower than 3 dB. For this reason, it could be concluded that the system is also insensitive to the modulation pattern, because for all the QAM modulations considered in the paper, the LINC output spectra look similar to the one shown in Fig. 2.

On the other hand, in Fig. 3, the influence of the A_x parameter in the system performances is shown. Notice that this parameter defines the appropriate value of the amplitude of the phase modulated signals $S_1(t)$ and $S_2(t)$. As shown in Table I, the lower the A_x value is, the higher the amplitude ($V/2$) of the phase modulated signals. From the figure it can be seen that no gain is obtained by decreasing the A_x value; that is, increasing V . Therefore, from now on we will maintain for A_x a conservative value of 0.9.

Taking into account that in practical situations U_R values greater than 50 dB could be needed, from this figure it can also be seen that to guarantee these performances, gain imbalance values as low as 0.1 dB are required.

Finally, the evolution of the adjacent channel rejection against the gain imbalance using the normalized guard band as parameter is shown in Fig. 4. In this figure, it is shown how the adjacent channel rejection increases approximately 0.5 dB every time the normalized guard band increases 0.1, irrespective of the gain imbalance value.

In summary, considering the results shown above, the following upper bounds, with a maximum error of 3 dB, could be put forward to characterize the system performances:

1. 4-QAM:

$$U_R(dB) \geq 32 \cdot 5 - 19 \cdot 2 \cdot \log_{10}(\Delta G) + 5 \cdot (\Delta B_g T)$$

2. 16-QAM:

$$U_R(dB) \geq 32 \cdot 0 - 19 \cdot 0 \cdot \log_{10}(\Delta G) + 7 \cdot (\Delta B_g T)$$

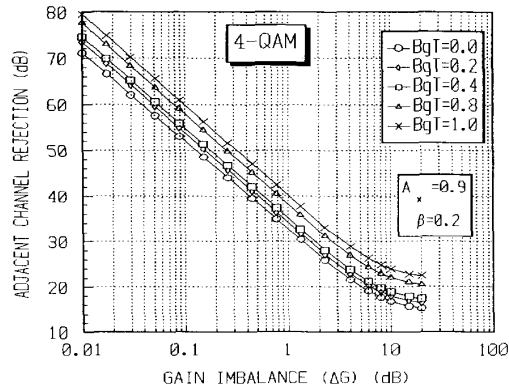


Fig. 4. Adjacent channel rejection versus the gain imbalance for 4-QAM modulation pattern with the normalized guard band as parameter.

3. 64-QAM:

$$U_R(\text{dB}) \geq 28 \cdot 5 - 19 \cdot 0 \cdot \log_{10}(\Delta G) + 7 \cdot (\Delta B_g T)$$

ΔG being the gain imbalance in dB, and $\Delta B_g T$ the normalized guard band ranging between 0 and 1.

B. Phase Imbalance

If the two path signals have two different delay values at the input of the combiner, the signals do not combine in phase, and this results again in a high degree of distortion.

Following the same method used for the gain imbalance, the evolution of the adjacent channel rejection against the phase imbalance, $\Delta\phi$, has also been studied. From the obtained results, it can newly be concluded that the system performances are very insensitive to the modulation type. Again, this can be explained noticing that 4, 16, and 64 QAM spectra of $S(t)$ for different phase imbalances are very similar, and consequently, the same behavior can be expected. On the other hand, when the effect of the roll-off factor in the system performances is considered, it may be noticed that the system also remains insensitive to the value of the roll-off coefficient.

It is also important to emphasize that even small phase imbalances are able to produce high degrading effects on the system performances. For example, a system with only one degree of phase imbalance has an adjacent channel rejection of around 50 dB, but if the phase imbalance increases up to 5 degrees, then adjacent channel rejection decreases to only 33 dB.

Finally, the evolution of the adjacent channel rejection against the phase imbalance using the normalized guard band as parameter is shown in Fig. 5. As in the gain imbalance case, it can be seen in this figure that the adjacent channel rejection increases approximately 0.5 dB every time the normalized guard band increases 0.1, independently of the phase imbalance value.

Similarly to the procedure followed for gain imbalances, we are also able to obtain the system performance upper bounds

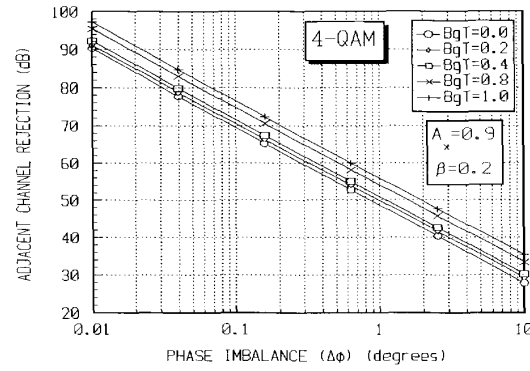


Fig. 5. Adjacent channel rejection versus the phase imbalance for 4-QAM modulation pattern with the normalized band guard as parameter.

when phase imbalances up to 5 degrees are considered. These upper bounds could be expressed as

1. 4-QAM:

$$U_R(\text{dB}) \geq 48 \cdot 0 - 20 \cdot 5 \cdot \log_{10}(\Delta\phi) + 5 \cdot (\Delta B_g T)$$

2. 16-QAM:

$$U_R(\text{dB}) \geq 45 \cdot 4 - 20 \cdot 75 \cdot \log_{10}(\Delta\phi) + 7 \cdot (\Delta B_g T)$$

3. 64-QAM:

$$U_R(\text{dB}) \geq 44 \cdot 5 - 21 \cdot 2 \cdot \log_{10}(\Delta\phi) + 7 \cdot (\Delta B_g T)$$

with $\Delta\phi$ in degrees.

IV. EFFECTS OF THE IMBALANCES ON THE BIT ERROR RATE

The effects of these imbalances on the bit error probability are further analyzed. In order to emphasize the influence of the imbalances, a system free of the intersymbol interference problem induced by the channel is considered; that is, a Nyquist equivalent impulse response is assumed. Then, at the output of the coherent demodulator, the in-phase, $r_x(t_0)$, and the quadrature, $r_y(t_0)$, components at the sampling instant, can be expressed as:

$$\left. \begin{aligned} r_x(t_0) &= k_0 \cdot [p(t_0) + k_1 \cdot q(t_0) \\ &\quad - k_1 \cdot \gamma_1(t_0) - k_2 \cdot \gamma_2(t_0)] + n_f(t_0) \\ r_y(t_0) &= k_0 \cdot [q(t_0) - k_1 \cdot p(t_0) \\ &\quad - k_1 \cdot \gamma_2(t_0) + k_2 \cdot \gamma_1(t_0)] + n_q(t_0) \end{aligned} \right\} \quad (4)$$

where:

$$\begin{aligned} p(t_0) &= x(t) * h_N^{0.5}(t)|_{t=t_0} \\ &= \sum_{k=-\infty}^{\infty} a_k \cdot h_N(t - kT)|_{t=t_0} = a_0 \\ q(t_0) &= y(t) * h_N^{0.5}(t)|_{t=t_0} \end{aligned}$$

$$\begin{aligned}
 &= \sum_{k=-\infty}^{\infty} b_k \cdot h_N(t - kT)|_{t=t_0} = b_0 \\
 \gamma_1(t) &= [C(t) \cdot X(t)] * h_N^{0.5}(t) \\
 \gamma_2(t) &= [C(t) \cdot y(t)] * h_N^{0.5}(t)
 \end{aligned} \quad (5)$$

being $h_N(t)$, the raised cosine Nyquist pulse,

$$\begin{aligned}
 k_0 &= \frac{1}{2} \cdot (1 + \Delta G \cdot \cos \Delta \phi), \\
 k_1 &= \frac{\Delta G \cdot \sin \Delta \phi}{1 + \Delta G \cdot \cos \Delta \phi}, \\
 k_2 &= \frac{1 - \Delta G \cdot \cos \Delta \phi}{1 + \Delta G \cdot \cos \Delta \phi},
 \end{aligned} \quad (6)$$

and n_f , and n_q are respectively the I and Q values of noise at sampling instant. In the above expression, perfect carrier and timing recovery have been assumed, and therefore, there is no intersymbol interference.

In order to estimate the bit error probability, the quasi-analytic method [9] has been used. For a specified power of white Gaussian noise at the threshold detector input, the error probability of the i th symbol with respect to the in-phase channel could be evaluated as in (7), found at the bottom of the page, where γ_{xi} is the i th received sample and S_{i1}^x and S_{i2}^x are the lower and upper thresholds. An equivalent expression could be obtained for the quadrature channel 1. After some algebraic operations, we can obtain the expression for the noise variance found at the bottom of the page (8).

The total bit error probability for a sequence of N symbols is computed as:

$$P_b(\epsilon) = \frac{1}{\log_2 M} \cdot \frac{1}{N} \sum_{i=1}^N (P_{e_i}^x + P_{e_i}^y - P_{e_i}^x P_{e_i}^y) \quad (9)$$

where M is the number of constellation points. A Gray encoding process has also been considered, with the result of only one bit error for each symbol error.

V. RESULTS

To characterize the influence on the bit error probability of the gain and phase imbalances, the increment on the SNR necessary to guarantee a fixed BER has been computed. In particular, the values 10^{-3} and 10^{-6} , as representative targets for voice and data transmission have been considered.

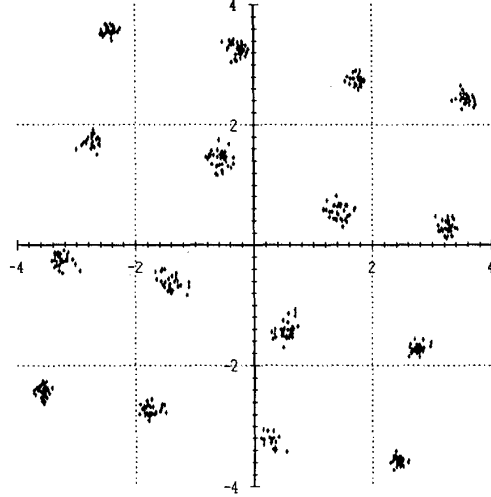


Fig. 6. Received constellation diagram for 16-QAM with 1.5 dB gain imbalance.

A. Gain Imbalances

When only gain imbalance is considered, $k_1 = 0$ and $k_2 \neq 0$ in expression (4). From this expression, it may be noticed that the received in-phase component depends on $\gamma_2(t)$, which is directly dependent on the quadrature component, as shown in (5). This cross-talk between the in-phase and quadrature channels leads to an important effect of rotation on the received signal constellation, as can be seen for 16 QAM with 1.5 dB of gain imbalance in Fig. 6. This effect can be compensated at the receiver by using a standard carrier recovery circuit.

Considering a roll-off factor equal to 0.2 and a BER value of 10^{-3} , the increment on the SNR needed to compensate a gain imbalance between the two RF paths is shown in Fig. 7(a). In this figure, the results corresponding to both systems with and without phase carrier optimization are depicted. From the obtained results, it can be concluded that the higher the modulation order, the more sensitive is the modulation for the gain imbalance. For example, for a 4-QAM modulation pattern, the system is almost insensitive when the phase optimization is performed, and if it is not performed, the system only needs an increment of about 2 dB at most in the SNR to cope with 2 dB of gain imbalance between both RF branches. If 16-QAM modulation is considered, with the same increment in the SNR, the system is able to cope with gain imbalance values equal to 3 dB and 0.5, depending

$$P_{e_i}^x = \begin{cases} \frac{1}{2} \operatorname{erfc} \left[\frac{\operatorname{Abs}(\gamma_{xi}) - S_{i1}^x}{\sigma_n \sqrt{2}} \right], & i = \pm(2N - 1) \\ \frac{1}{2} \operatorname{erfc} \left[\frac{\operatorname{Abs}(\gamma_{xi}) - S_{i1}^x}{\sigma_n \sqrt{2}} \right] + \operatorname{erfc} \left[\frac{S_{i2}^x - \operatorname{Abs}(\gamma_{xi})}{\sigma_n \sqrt{2}} \right], & i = \pm 1, \pm 3, 2 \dots \pm (2N - 3) \end{cases} \quad (7)$$

$$\sigma_n^2 = \frac{(1 + K_1^2) \frac{M-1}{3} + (K_1^2 + K_2^2) \overline{\gamma_1^2(t_0)} - 2K_1(1 + K_2) \overline{a_0 \gamma_1(t_0)}}{\operatorname{SNR}} \quad (8)$$

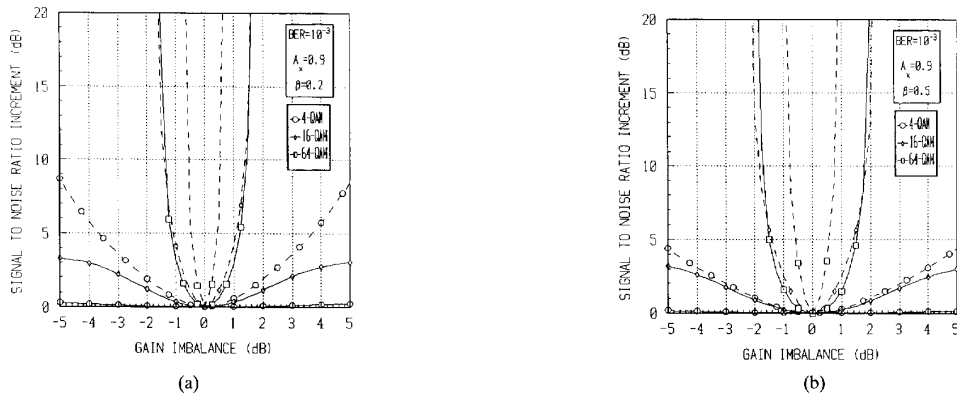


Fig. 7. Increment of the SNR as function of the gain imbalance for a pre-fixed BER equal to 10^{-3} . Dashed lines indicate no carrier recovery circuit considered. Roll-off factor equal to : (a) 0.2, (b) 0.5.

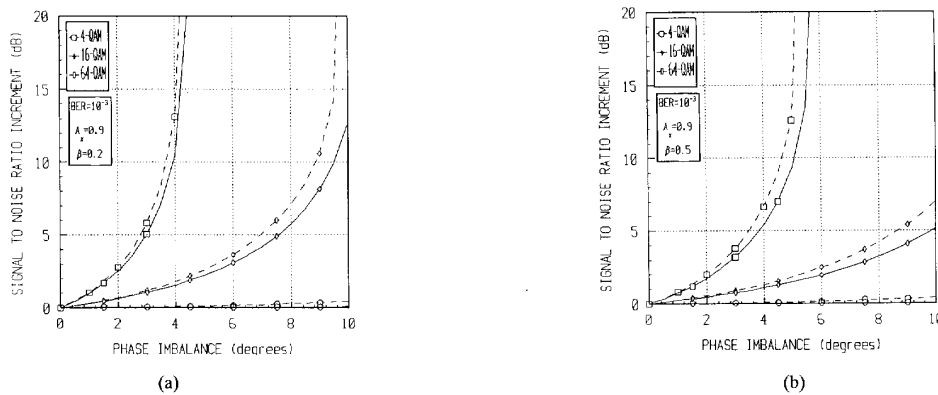


Fig. 8. Increment of the SNR as a function of the phase imbalance for a pre-fixed BER equal to 10^{-3} . Dashed lines indicate no carrier recovery circuit considered. Roll-off factor equal to : (a) 0.2, (b) 0.5.

on the presence or absence of the carrier recovery circuit. Finally, for 64-QAM modulation, these values reduce to 0.6 and 0.2, respectively. Notice that for a gain imbalance of 1.2 dB (10% approximately), the 64-QAM modulation degrades in approximately 6 dB the SNR needed to guarantee a BER of 10^{-3} ; that is, with respect to an ideal LINC transmitter, it is necessary to increase four times the value of the transmitted power to maintain the same system quality. Similar results are obtained for a BER of 10^{-6} .

When a roll-off factor equal to 0.5 is considered, the obtained results are shown in Fig. 7-b. In this case, the system performance is slightly better than the obtained results, considering a roll-off factor equal to 0.2; but in general, the same ideas and conclusions obtained before apply in this case.

Finally, it is also important to emphasize that the conclusions obtained in the previous paragraph could be extended to other BER's.

B. Phase Imbalance

Fig. 8 shows the evolution of the increment in the SNR needed to compensate the effect of the phase imbalance for the same roll-off values. This figure shows only positive values of the phase imbalance because negative values produce the

same results. On the other hand, looking at the expression (4), when only the phase imbalance is considered, then $K_1 \neq 0$ and $K_2 \neq 0$, and as a result, the cross-talk between the in-phase and the quadrature channels appears. For this reason, results considering two situations have been obtained. In the first case, the carrier recovery loop is able to compensate for this effect, [10], but in the second case, it is not. Again, from the obtained results, it could be concluded that the higher the modulation order, the more sensitive the modulation to the phase imbalance. For a BER value equal to 10^{-3} and 4-QAM modulation pattern, the system only needs an increment of 0.1 dB in the SNR to cope with values of phase imbalance as high as 10 degrees between the two RF channels when no cross-talk appears, and 0.2 dB if cross-talk is considered. However, when 16-QAM modulation is taken into account, for a 3-dB increment in the SNR, the system is able to cope with a phase imbalance value equal to 6 degrees if a received signal without cross-talk is considered, but it is only able to cope with up to 5 degrees in the case of cross-talk; while for 64-QAM modulations, with the above mentioned SNR increment, the maximum phase imbalance values reduce to only 2.3 and 2 degrees, respectively. Similar results are obtained for a bit error value of 10^{-6} .

TABLE II
INCREMENT OF THE SNR AS FUNCTION OF THE GAIN IMBALANCE (a), AND THE PHASE IMBALANCE (b), FOR A PREFIXED BER EQUAL TO 10^{-4} . COMPARISON BETWEEN A CONVENTIONAL QAM MODULATOR, [8], AND A LINC TRANSMITTER

	4-QAM		16-QAM		64-QAM	
	QAM MOD.	LINC	QAM MOD.	LINC	QAM MOD.	LINC
G=-1.5dB	0.4dB	0.05dB	3.0dB	0.8dB	>10dB	11dB
G=-1.0dB	0.2dB	0.05dB	1.8dB	0.4dB	9dB	2.8dB
G=-0.5dB	0.1dB	0.05dB	0.5dB	0.1dB	3dB	0.5dB
G=0.5dB	0.1dB	0.05dB	0.2dB	0.1dB	2dB	1dB
G=1.0dB	0.2dB	0.05dB	0.9dB	0.4dB	6dB	2.7dB
G=1.5dB	0.4dB	0.05dB	1.8dB	0.8dB	>10dB	8.6dB

(a)

	4-QAM		16-QAM		64-QAM	
	QAM MOD.	LINC	QAM MOD.	LINC	QAM MOD.	LINC
F=2°	0.1dB	0.1dB	0.1dB	0.5dB	0.4dB	2dB
F=4°	0.1dB	0.1dB	0.3dB	1dB	1.5dB	6dB
F=6°	0.1dB	0.1dB	1dB	2dB	2.5dB	>10dB
F=8°	0.2dB	0.1dB	1.5dB	3.5dB	4.2dB	>10dB
F=10°	0.3dB	0.2dB	1.9dB	5.8dB	6.5dB	>10dB

(b)

Considering a roll-off factor equal to 0.5, the increment on the SNR needed to compensate for the phase imbalance is shown in Fig. 8(b). The figure also shows the sensitivity of 64-QAM modulation as regards the phase imbalances, in comparison to the 4-QAM modulation that is able to cope with up to ± 10 degrees of the phase imbalance value with a SNR degradation lower than 0.2 dB. However, for 64-QAM modulation, the phase imbalance cannot be greater than 3 degrees to maintain degradation lower than 3 dB on the SNR.

Finally, it is worthwhile to compare the sensitivity of a LINC transmitter to a conventional QAM modulator. In Table II a comparison between the results obtained in [8] for a conventional QAM modulator and these obtained for the LINC transmitter is presented. In Table II(a) it can be seen that the LINC transmitter is less sensitive to the gain imbalances for all the modulation patterns. However, the conventional QAM modulator presents a better behavior for phase imbalances, as is shown in Table II(b). In any case, it must be remembered that in the conventional QAM modulator, completely linear filtering and power amplification are assumed; whereas, the LINC transmitter allows the use of highly non-linear power amplifiers working close to its saturation point and, as a result, to increase the system power efficiency.

VI. CONCLUSIONS

In this paper, the effect of the RF signal processing impairments in a LINC transmitter has been analysed. In particular 4, 16, and 64 QAM modulation patterns with raised cosine Nyquist filtering and two different kinds of path imbalances are considered. First of all, the system degradations are described in terms of the adjacent channel rejection, and analytical upper bounds have been obtained for all the analyzed cases. Mainly, the gain imbalance between both power amplifiers, but also the phase imbalance, appears as a serious limitation of the performances of the LINC transmitter.

The influence of the RF imbalances on the bit error probability has also been analyzed. From the obtained result it can be concluded that 4-QAM modulation remains almost insensitive to the effect of those imbalances. The same applies for 16 QAM, in case the imbalances remain below reasonable limits. On the contrary, since 64-QAM or higher modulations are very sensitive to the effect of these imbalances, careful implementations are required.

ACKNOWLEDGMENT

The authors wish to acknowledge the anonymous reviewers for their suggestions which have led to improvements in the work.

REFERENCES

- [1] R. Steele, "Deploying personal communication networks," *IEEE Commun.*, pp. 12-15, Sept. 1990.
- [2] J. Yamas, "An HF dynamic range amplifier using feedforward techniques," *RF Design*, pp. 50-59, July 1987.
- [3] V. Petrovic, "Application of Cartesian feedback to HF SSB transmitters," in *Proc. Inst. Elect. Eng. Conf. on H.F.: Commun. Syst. Techniques*, pp. 81-85, 1985.
- [4] A. A. Saleh and J. Salz, "Adaptive linearization of power amplification in digital radio systems," *Bell System Technical J.*, pp. 1019-1033, Apr. 1983.
- [5] D. C. Cox, "Linear amplification with non-linear components," *IEEE Trans. Commun.*, pp. 1942-1945, Dec. 1974.
- [6] S. A. Hetzel, A. Bateman, and J. P. McGeehan, "A LINC transmitter," in *Proc. 41st IEEE Veh. Technol. Conf.*, St. Louis, MO, pp. 133-137.
- [7] F. Casadevall, J. J. Olmos, "On the behavior of the LINC transmitter," in *Proc. 40th IEEE Veh. Technol. Conf.*, May 6-9, 1990, Orlando, FL, pp. 20-34.
- [8] H. Sari, G. Karam, "Compensation of modem imperfections by adaptive filtering," in *Proc. GLOBECOM '86*, 1986, pp. 511-516.
- [9] M. J. Jeruchim, "Techniques for estimating the bit error rate in the simulation of digital communication systems," *IEEE J. Select. Areas Commun.*, vol. SAC-2, pp. 153-170, Jan. 1984.
- [10] S. Moridi, H. Sari, "Analysis of decision-feedback carrier recovery loops with application to 16-QAM digital radio systems," in *Proc. Int. Conf. Commun. (ICC '83)*, 1983, pp. 671-675.



Fernando J. Casadevall (M'87) was born in Barcelona, Spain, in 1955. He received the Engineer of Telecommunication and Ph.D. degrees from the Escola Tècnica Superior d'Enginyers de Telecomunicació de Barcelona (ETSETB), Universitat Politècnica de Catalunya (UPC), Spain, in 1977 and 1983, respectively.

In 1978 he joined the ETSETB, where he was an Associate Professor from 1983 to 1991. He is currently a Professor in the Signal Theory and Communications Department, UPC. His research interests include equalization techniques for digital fiber optic systems and digital communications, with particular emphasis on digital radio and its performance under multipath propagation conditions, especially cellular and personal communication systems, multipath receiver design, and digital signal processing. He is actively participating in the European research programs COST231 and RACE.



Antonio Valdovinos was born in Barbastro, Spain, in 1966. He received the Engineer of Telecommunication degree from the Escola Tècnica Superior d'Enginyers de Telecomunicació de Barcelona (ETSETB), Universitat Politècnica de Catalunya (UPC), Spain, in 1990. In 1991 he joined, under a research grant, the Signal Theory and Communications Department, UPC, Spain, where he is currently pursuing the Ph.D. degree in the area of mobile radio communication systems.

Presently, he is an Assistant Professor in the UPC.